Cardiovascular Drugs and Therapy (2019) 33:13–23
https://doi.org/10.1007/s10557-018-06848-8

ORIGINAL ARTICLE

Inhibition of Phosphoglycerate Mutase 5 Reduces Necroptosis in Rat Hearts Following Ischemia/Reperfusion Through Suppression of Dynamin-Related Protein 1

Lang She[1] · Hua Tu[1] · Yin-Zhuang Zhang[2] · Li-Jing Tang[1] · Nian-Sheng Li[1,3] · Qi-Lin Ma[2] · Bin Liu[4] · Qingjie Li[5] · Xiu-Ju Luo[3] · Jun Peng[1,4]

Published online: 14 January 2019

Abstract

Purpose Necroptosis is an important form of cell death following myocardial ischemia/reperfusion (I/R) and phosphoglycerate mutase 5 (PGAM5) functions as the convergent point for multiple necrosis pathways. This study aims to investigate whether inhibition of PGAM5 could reduce I/R-induced myocardial necroptosis and the underlying mechanisms.

Methods The SD rat hearts (or H9c2 cells) were subjected to 1-h ischemia (or 10-h hypoxia) plus 3-h reperfusion (or 4-h reoxygenation) to establish the I/R (or H/R) injury model. The myocardial injury was assessed by the methods of biochemistry, H&E (hematoxylin and eosin), and PI/DAPI (propidium iodide/4′,6-diamidino-2-phenylindole) staining, respectively. Drug interventions or gene knockdown was used to verify the role of PGAM5 in I/R (or H/R)-induced myocardial necroptosis and possible mechanisms.

Results The I/R-treated heart showed the injuries (increase in infarct size and creatine kinase release), upregulation of PGAM5, dynamin-related protein 1 (Drp1), p-Drp1-S616, and necroptosis-relevant proteins (RIPK1/RIPK3, receptor-interacting protein kinase 1/3; MLKL, mixed lineage kinase domain-like); these phenomena were attenuated by inhibition of PGAM5 or RIPK1. In H9c2 cells, H/R treatment elevated the levels of PGAM5, RIPK1, RIPK3, MLKL, Drp1, and p-Drp1-S616 and induced mitochondrial dysfunctions (elevation in mitochondrial membrane potential and ROS level) and cellular necrosis (increase in LDH release and the ratio of $PI^+/DAPI^+$ cells); these effects were blocked by inhibition or knockdown of PGAM5.

Conclusions Inhibition of PGAM5 can reduce necroptosis in I/R-treated rat hearts through suppression of Drp1; there is a positive feedback between RIPK1 and PGAM5, and PGAM5 might serve as a novel therapeutic target for prevention of myocardial I/R injury.

Keywords Ischemia/reperfusion · Necroptosis · Phosphoglycolic acid · Phosphoglycerate mutase 5 (PGAM5) · Dynamin-related protein 1(DRP1)

Lang She and Hua Tu contributed equally to this work.

Electronic supplementary material The online version of this article (https://doi.org/10.1007/s10557-018-06848-8) contains supplementary material, which is available to authorized users.

✉ Xiu-Ju Luo
xjluo22@csu.edu.cn

✉ Jun Peng
Junpeng@csu.edu.cn

[1] Department of Pharmacology, Xiangya School of Pharmaceutical Sciences, Central South University, No.110 Xiangya Road, Changsha 410078, China

[2] Department of Cardiovascular Medicine, Xiangya Hospital, Central South University, Changsha 410008, China

[3] Department of Laboratory Medicine, Xiangya Third Hospital, Central South University, Changsha 410013, China

[4] Hunan Provincial Key Laboratory of Cardiovascular Research, Xiangya School of Pharmaceutical Sciences, Central South University, Changsha 410078, China

[5] Department of Internal Medicine, The University of Texas Medical Branch at Galveston, Galveston, TX 77555-1083, USA

Introduction

It is well established that myocardial ischemia/reperfusion (I/R) results in cardiac cell necrosis and apoptosis [1–3]. For a long time, cell death has been divided into two types: accidental death and regulated death. Apoptosis is the first-identified type of regulated cell death [4, 5]. In contrast, necrosis is considered to be a random, passive cell death without definable mediators [6, 7]. However, this long-standing dogma regarding cell death has recently been challenged and overturned by the recognition that necrosis can also be a regulated process [8, 9]. To date, multiple forms of regulated necrosis have been identified and reported, including necroptosis, ferroptosis, pyroptosis, oxytosis, and cyclophilin D–mediated necrosis [8, 10–12]. Among them, necroptosis is the most well-known form of regulated necrosis.

Necroptosis is the most defined regulated necrosis that requires RIPK1/RIPK3 (receptor-interacting protein kinase 1/3) and MLKL (mixed lineage kinase domain-like) [13], and the RIPK1/RIPK3/MLKL pathway–mediated necroptosis under multiple conditions is well recognized [14–16]. Recent studies have shown that necroptosis is one of the main forms of cell death following myocardial I/R [17–20]. There is evidence that intervention in signaling pathways involved in necroptosis could ameliorate the myocardial I/R injury [19], opening a new direction for the amelioration of I/R injury through targeting the molecules that mediate necroptosis.

Phosphoglycerate mutase family member 5 (PGAM5) is a mitochondrial membrane protein that functions as an atypical Ser/Thr phosphatase [21, 22]. In a TNF-α-induced necrosis model of HeLa cells, PGAM5 was identified as a component of the RIPK1- and RIPK3-containing protein complexes. Upon induction of necrosis, PGAM5 recruits Drp1 (dynamin-related protein 1), a key protein for regulating mitochondrial fission, and activates it by dephosphorylating the serine residue at the site of 637 [23]. Activation of Drp1 may cause mitochondrial fragmentation, leading to mitochondrial dysfunction, an early and obligatory step for necrosis execution [21]. It is not known, however, whether PGAM5 involves in I/R-induced myocardial necroptosis and whether inhibition of PGAM5 could reduce myocardial I/R injury.

The purpose of this study was to explore the role of PGAM5 in myocardial I/R injury and to elucidate the underlying mechanisms. By using a rat model of myocardial I/R injury and a PGAM5 inhibitor, we examined the functional role of PGAM5 in RIPK1/RIPK3/MLKL-dependent necrosis. By using a cell model of hypoxia/reoxygenation (H/R) injury, we were able to verify that inhibition of PGAM5 could reduce necroptosis of cardiac cells through suppression of Drp1.

Materials and Methods

Animals

Male Sprague-Dawley (SD) rats (250–300 g) were provided by the Laboratory Animal Center, Xiangya School of Medicine, Central South University, China. All animals received humane care in compliance with the "Guide for the Care and Use of Laboratory Animals" published by the National Institutes of Health (NIH Publication, eighth edition, 2011) and the Animal Research: Reporting In Vivo Experiments (ARRIVE) guidelines. Experiments were approved by the Central South University Veterinary Medicine Animal Care and Use Committee.

Experimental Protocol for Animal Studies

The animals were randomly divided into 7 groups (n = 11 in each group): (1) the control group, no treatment; (2) the sham group, rats underwent surgical procedures without ischemic insult; (3) the I/R group, rats were subjected to 1 h of ischemia followed by 3 h of reperfusion; (4) and (5) the PGAM5 inhibitor at low- or high-dose group, rats were treated with PGA (phosphoglycolic acid, dissolved in H_2O, purchased from J&K Scientific LTD, China) at 10 or 30 mg/kg (i.v.) 30 min before reperfusion; (6) the Nec-1 group, rats were treated with Nec-1 (necrostatin-1, served as a positive control for necroptosis, purchased from Santa Cruz, USA) at 20 mg/kg (i.p.) 30 min prior to reperfusion. Nec-1 was dissolved in vehicle (DMSO: corn oil = 1:99, *v*/*v*); and (7) the vehicle group, rats were treated with equal volume of Nec-1 vehicle 30 min before reperfusion. The surgical procedure for I/R was performed as previously described [24]. At the end of reperfusion, 8 hearts from each group were saved for infarct size measurement, whereas the remaining 3 hearts from each group were collected for Western blot analysis.

Experimental Protocol for Cell Studies

Rat heart–derived H9c2 cells were cultured at constant density ($1 \times 10^4/cm^2$) and grown to 70~80% confluency in DMEM with 10% fetal bovine serum. Cells were rinsed with PBS and rendered quiescent in serum-free DMEM for 12 h before the experiment. H9c2 cells were allocated to six groups (6 individual experiments per group): (1) the control group, H9c2 cells were cultured under normal condition; (2) the H/R group, H9c2 cells were subjected to 10-h hypoxia ($O_2/N_2/CO_2$, 1:94:5) in preconditioned hypoxic medium plus 4-h reoxygenation; (3) and (4) the PGAM5 inhibitor at low- or high-dose group, PGA was given to culture medium (3 μM or 10 μM) at the beginning of H/R; (5) the Nec-1 group, Nec-1 was added to culture medium (10 μM) at the beginning of H/R; (6) the vehicle group, equal volume of DMSO (0.1%, final

concentration) was given to culture medium right at the beginning of H/R.

To verify the role of PGAM5 in promotion of necroptosis in H/R-treated H9c2 cells, PGAM5 was knocked down with siRNA. H9c2 cells were divided into 4 groups ($n = 6$ in each group): (1) the control group, (2) the H/R group, (3) the H/R + PGAM5 siRNA group (cells were transfected with PGAM5 siRNAs and subjected to H/R), and (4) the H/R + siRNA NC group (cells were transfected with scrambled siRNAs and subjected to H/R).

Knockdown of PGAM5 in H9c2 Cells

The siRNAs specific to the rat PGAM5 gene were provided by Guangzhou RiboBio Co., Ltd. (Guangzhou, China), and they were transfected into H9c2 cells by using Lipofectamine™ 2000 (Invitrogen, Carlsbad, CA). In brief, 100 pmol of siRNAs and 5.0 μl of Lipofectamine™ 2000 was mixed in 500 μl of culture medium and kept at room temperature for 15~20 min. The cells were harvested 48 h after the transfection and they were subjected to the follow-up experiments. The efficiency of gene knockdown was evaluated by real-time PCR and Western blot. Scrambled siRNAs were used as a negative control.

Measurement of Infarct Size

Blood samples (3 ml from each rat) were collected at the end of reperfusion and the plasma was isolated for relevant studies. The left coronary was ligated, and 1 ml of Evans blue (10 mM) was injected into the left ventricular cavity to perfuse the non-ischemic parts of the heart. The heart was cut into pieces; then, the atrial tissue, right ventricle, and Evans blue–stained LV were resected. The remaining LV was sliced into sections (1 mm thickness) from the apex to the base. The slices were incubated with 1% triphenyltetrazolium chloride (TTC) solution away from light at 37 °C for 15 min to stain the viable myocardium (brick red), and then, they were fixed in a 4% paraformaldehyde solution for 24 h. At the end, the slices were traced onto acetate sheets and measured by an image software (ImageJ, National Institutes of Health, Bethesda, MD, USA). The infarct area was presented as the ratio of the infarct zone area to the risk zone size.

Creatine Kinase Activity Assay

Three milliliters of blood was collected for isolation of serum at the end of reperfusion via the carotid artery. The total serum creatine kinase activity was spectrophotometrically measured by using commercial kits according to the instructions provided by the supplier (Biosino Bio-Technology, Beijing, China).

Hematoxylin and Eosin Staining

Hematoxylin and eosin (HE) staining was performed to evaluate the morphological changes in cardiac tissues among different groups. In brief, LV tissues were fixed in 4% paraformaldehyde and embedded in paraffin, and then, they were cut into 5-μm-thick sections. The slices underwent hematoxylin and eosin staining for 20 and 2 min, respectively, following depleting wax. In the end, they were imaged with microscope (Nikon Eclipse 80i, Japan) to assess the morphological changes.

Western Blot Analysis

Cardiac tissues (infarct and border zone) and H9c2 cells were homogenized with ice-cold lysis buffer, and the concentration protein in homogenate was assayed by using a commercial kit (Beyotime, Nanjing, China). Western blot was carried out according to standard protocol. Briefly, samples containing ~ 40 μg of proteins were proceeded to 10% SDS-PAGE, and they were transferred to polyvinylidene fluoride (PVDF) membranes. The PVDF membranes were incubated with primary antibodies against RIPK1 (Santa Cruz Biotech, Santa Cruz, USA), RIPK3 (Abcam, Cambridge, USA), MLKL (Abcam, Cambridge, USA), PGAM5 (Santa Cruz Biotech, Santa Cruz, USA), Drp1 (Abcam, Cambridge, USA), and p-DRP1 ser-616 or ser-637 (cell signaling technology, Shanghai, China), and then, they were incubated with HRP-conjugated secondary antibodies. The protein signals were measured by Luminata Crescendo Western HRP substrate via Molecular Imager ChemiDoc XRS System (Bio-Rad, Philadelphia, PA). Densitometric quantification was carried out by ImageJ (NIH, USA). GAPDH (Beyotime, Jiangsu, China) served as loading controls. Arbitrary optical density units of the targeting proteins were normalized against control, and the results were expressed as fold change.

Assay of LDH Release

Culture medium was collected for assay of LDH release (an indicator of cellular necrosis) with a colorimetric assay kit (Beyotime, Jiangsu, China) following the protocol provided by the manufacturer. Released LDH was assayed with a coupled enzymatic reaction that leads to the conversion of a tetrazolium salt into a red color formazan by diaphorase. In brief, 120 μl of culture medium was mixed with 60 μl of LDH work solution, and then, they were incubated at 25~30 °C for 30 min. The absorbance was measured at 490 nm. The percent of LDH release was calculated following a formula offered by the manufacturer.

PI/DAPI Double Staining

Cardiac cell necrosis was also assessed by propidium iodide (BD 550825), which can stain the nuclei of cells with loss in integrity of the plasma membrane. H9c2 cells were rinsed twice with PBS, and then, they were incubated with PI dye solution (10 μg/ml) for 15 min at 37 °C. Subsequently, H9c2 cells were rinsed twice with PBS and fixed with 4% paraformaldehyde for 15 min. Then, H9c2 cells were counterstained with DAPI for 2 min and visualized under a fluorescence microscope (Olympus IX71, Tokyo, Japan). Twenty high-power fields were randomly chosen and blindly quantitated. The number of $PI^+/DAPI^+$ positive cells (necrotic cells) was expressed as percent of the total cells.

Measurement of Mitochondrial Membrane Potential

Mitochondrial membrane potential ($\Delta\Psi m$) was measured with commercial JC-1 kits (Beyotime, Jiangsu, China). Briefly, H9c2 cells were seeded into six-well plates and incubated with 2 ml of culture medium overnight. After replacing the culture with 1-ml JC-1 dye and 1-ml culture medium, the plates were returned to the incubator and cultured at 37 °C for 20 min. The cells were observed under a fluorescence microscope (Olympus IX71, Tokyo, Japan). Normal cells emit red-orange fluorescence in JC-1 aggregates, whereas the injured cells emit green fluorescence because of the JC-1 monomers in the cytoplasm.

Determination of Reactive Oxygen Species Levels

The assay of intracellular reactive oxygen species (ROS) levels depends on the fluorescent signal of 2,7-dichlorodihydrofluorescein diacetate (DCFH-DA), which is a cell-permeable indicator for ROS (Beyotime, Jiangsu, China). DCFH-DA is non-fluorescent until the acetate groups are removed by intracellular ROS. In brief, H9c2 cells were rinsed with PBS and incubated with 10 μM of DCFH-DA for 20 min at 37 °C. Then, the ROS-mediated fluorescence was visualized under a fluorescent microscope with excitation/emission set at 502/523 nm. The quantification for fluorescent intensity (ROS level) was carried out with ImageJ. Arbitrary fluorescent units were normalized against control and expressed as fold change.

Statistics

The statistical analysis was conducted by SPSS software (Version 20.0). The data were expressed as mean ± SEM. Differences among multiple groups were examined by the analysis of variance with Bonferroni's multiple comparison tests. Differences were regarded as significant when $P < 0.05$.

Results

Inhibition of PGAM5 Ameliorated Myocardial I/R Injury

HE staining for cardiac tissues showed fiber loss and disarray in the I/R group; these effects were attenuated by PGA (10 or 30 mg/kg, PGAM5 inhibitor) or Nec-1 (20 mg/kg, RIPK1 inhibitor) treatment (Fig. 1a). I/R led to 52.1 ± 3.2% infarct in the area at risk concomitant with a significant increase in serum CK activity (Fig. 1b, c). Pretreatment with PGA (10 or 30 mg/kg) or Nec-1 (20 mg/kg) caused an obvious reduction in infarct size together with a significant decrease in serum CK activity (Fig. 1b, c). Vehicle treatment did not show such cardioprotective effect. No significant difference in infarct size and morphological change was observed between the sham group and the control group. But the serum CK activity in the sham group was increased compared with that in the control group because of the surgical injury.

Inhibition of PGAM5 Suppressed I/R-Induced Necroptosis-Relevant Protein Expression

Necroptosis means cells can execute necrosis in a programmed fashion, and RIPK1, RIPK3, and MLKL are the components of the signaling pathway responsible for executing the necroptosis. As shown in Fig. 2, PGAM5 protein expression in rat heart was obviously upregulated following I/R, accompanied by an increase in protein levels of RIPK1, RIPK3, and MLKL. Pretreatment with PGA (10 or 30 mg/kg) suppressed the I/R-induced PGAM5 protein upregulation, accompanied by decreases in RIPK1, RIPK3, and MLKL protein levels. Interestingly, pretreatment with Nec-1 (20 mg/kg) also achieved similar results. Vehicle treatment had no such effect.

Inhibition of PGAM5 Reduced DRP1 and p-DRP1-S616 Protein Levels in Rat Hearts Following I/R

The mitochondrial fission protein DRP1 is supposed to be dephosphorylated by PGAM5 at the site of S637. As shown in Fig. 3a, DRP1 protein level was notably upregulated in I/R-treated rat heart concomitant with elevated levels of p-DRP1-S637 and p-DRP1-S616, inconsistent with the phosphatase function of PGAM5. As shown in Fig. 3b, DRP1 and p-DRP1-S616 protein levels in rat hearts were elevated following I/R. Pretreatment with PGA (10 or 30 mg/kg) obviously blocked the elevation of DRP1 and p-DRP1-S616 levels in I/R-treated rat hearts. Pretreatment with Nec-1 also showed similar results, whereas vehicle treatment had no effect.

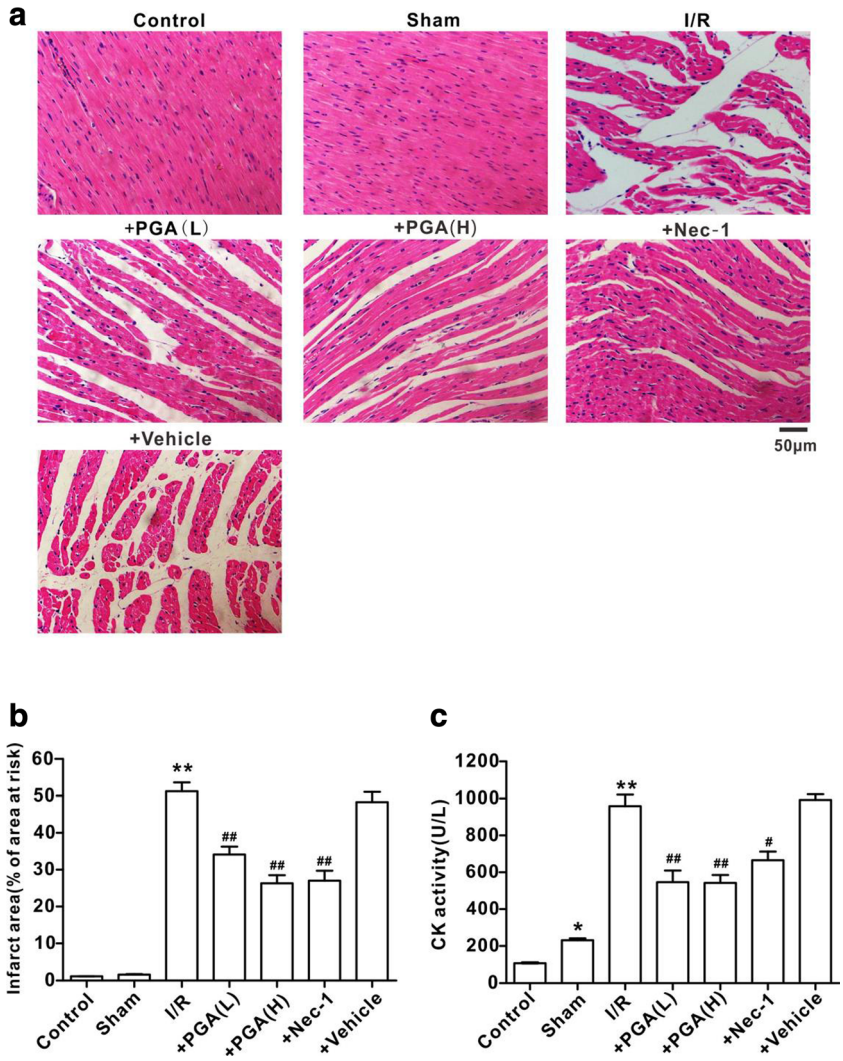

Fig. 1 Inhibition of PGAM5 attenuates myocardial I/R injury. **a** Representative images of HE staining in each group. In the I/R group, there was myocardial fiber loss and disruption, which was reversed by PGAM5 inhibitor. **b** Infarct size (expressed as percentage of the area at risk). **c** Serum creatine kinase (CK) activity. All values were expressed as mean ± SEM ($n = 8$ in each group). I/R: ischemia/reperfusion; +PGA: I/R + phosphoglycolic acid; +Nec-1: I/R + necrostatin-1. $^{*}P < 0.05$, $^{**}P < 0.01$ vs. sham, $^{\#}P < 0.05$, $^{\#\#}P < 0.01$ vs. I/R

Inhibition or Knockdown of PGAM5 Reduced the Levels of Necroptosis-Relevant Proteins, DRP1, and p-DRP1-S616 in H/R-Treated H9c2 Cells

In agreement with the results from I/R-treated rats, PGAM5 protein expression in H/R-treated H9c2 cells was evidently upregulated, concomitant with elevated protein levels of RIPK1, RIPK3, and MLKL (Fig. 4 and Fig. S1A–E). Inhibition or knockdown of PGAM5 significantly suppressed the H/R-induced PGAM5 protein expression, accompanied by a decrease in RIPK1, RIPK3, and MLKL protein levels. Pretreatment with RIPK1 inhibitor also gave rise to similar results, whereas the vehicle did not show such effect.

Consistent with the results from the I/R group, DRP1 and p-DRP1-S616 levels in H/R-treated H9c2 cells were obviously elevated (Fig. 4 and Fig. S1F–H). Inhibition or knockdown of PGAM5 abrogated the elevation of DRP1 and p-DRP1-S616 levels in H/R-treated H9c2 cells. Administration of RIPK1 inhibitor also achieved similar results, but the vehicle or siRNA negative control had no such effect.

Inhibition or Knockdown of PGAM5 Improved Mitochondrial Function

$\Delta\Psi m$ and ROS levels are well-known parameters for evaluation of mitochondrial function. As displayed in Fig. 5a and Fig. S2A, the green signals in H/R-treated H9c2 cells were much stronger than those in the control cells, suggesting an obvious reduction in $\Delta\Psi m$. There was also a significant increase in ROS levels (Fig. 5b and Fig. S2B). Inhibition or knockdown of PGAM5 obviously weakened the green signals compared to those in the H/R-treated cells accompanied by a decrease in ROS production. RIPK1 inhibitor also showed similar effect, whereas the vehicle or siRNA negative control did not affect mitochondrial function.

Inhibition or Knockdown of PGAM5 Decreased Necrosis in H/R-Treated H9c2 Cells

A cell model of H/R injury was established to verify the findings in vivo. Cellular necrosis was evaluated by PI/DAPI

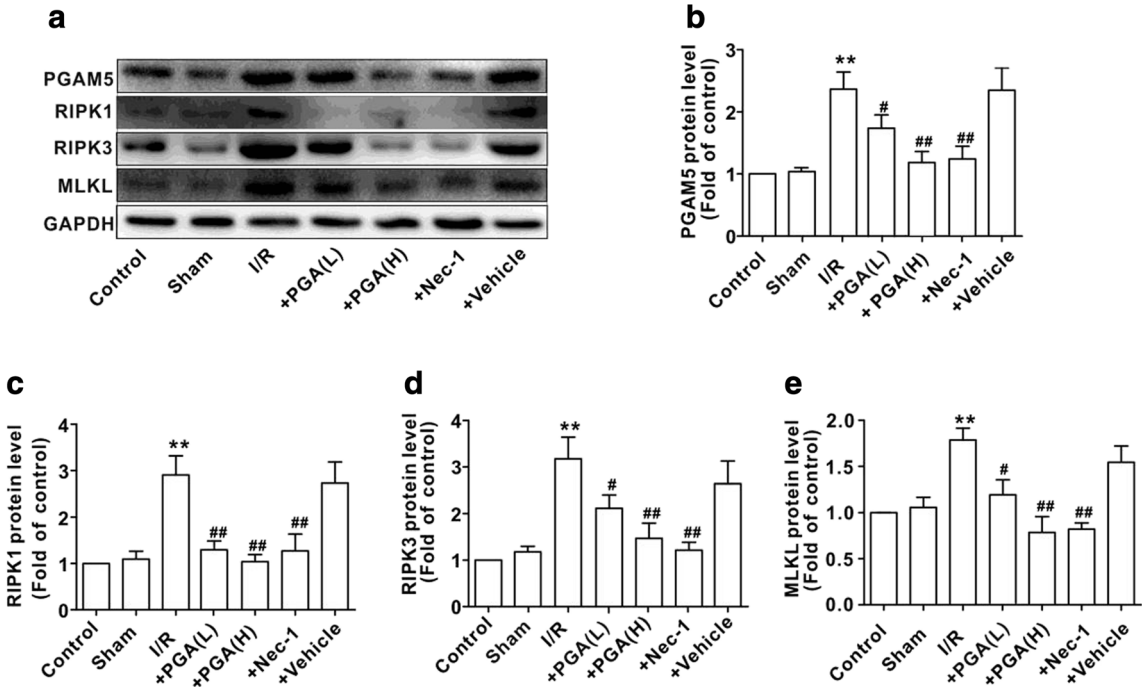

Fig. 2 Inhibition of PGAM5 downregulates necroptosis-relevant protein expression in I/R-treated rat hearts. Arbitrary optical density units of the targeting protein were normalized against GAPDH and expressed as fold change. **a** Representative images of Western blot results for each protein. **b** PGAM5 protein level. **c** RIPK1 protein level. **d** RIPK3 protein level. **e** MLKL protein level. All values were expressed as mean ± SEM (3 independent experiments in each group). I/R: ischemia/reperfusion; +PGA: I/R + phosphoglycolic acid; +Nec-1: I/R + necrostatin-1. $^{**}P < 0.01$ vs. sham, $^{\#}P < 0.05$, $^{\#\#}P < 0.01$ vs. I/R

double staining or LDH release. As displayed in Fig. 6 and Fig. S3, comparing to the control group, necrotic cells (PI^+/$DAPI^+$ cells) in the H/R group were obviously increased (Fig. 6a, b), accompanied by an increase in LDH release (Fig. 6c). Inhibition of PGAM5 blocked the necrosis in H/R-treated H9c2 cells, as did the RIPK1 inhibitor, whereas the vehicle

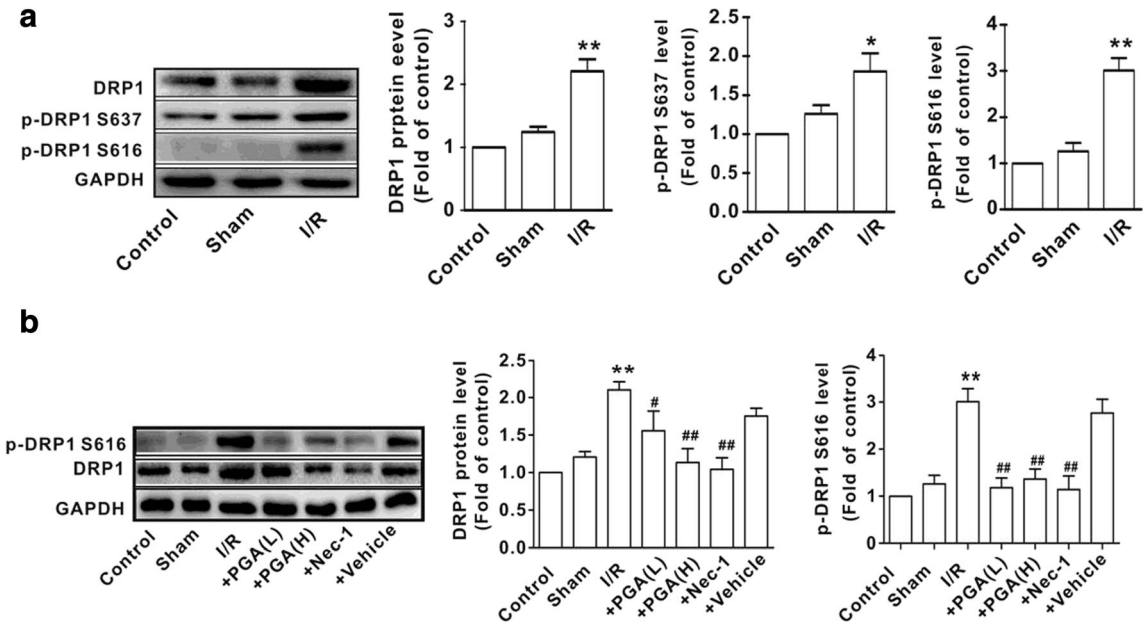

Fig. 3 Inhibition of PGAM5 reduces DRP1 and p-DRP1-S616 levels in I/R-treated rat hearts. Arbitrary optical density units of the targeting protein were normalized to GAPDH and expressed as fold change. **a**, **b** Representative images of Western blot results for each protein. Left panel, DRP1 protein level; middle panel, p-DRP1-S637 protein level; right panel, p-DRP1-S616 protein level. All values were expressed as mean ± SEM (3 independent experiments in each group). I/R: ischemia/reperfusion; +PGA: I/R + phosphoglycolic acid; +Nec-1: I/R + necrostatin-1. $^{*}P < 0.05$, $^{**}P < 0.01$ vs. sham, $^{\#}P < 0.05$, $^{\#\#}P < 0.01$ vs. I/R

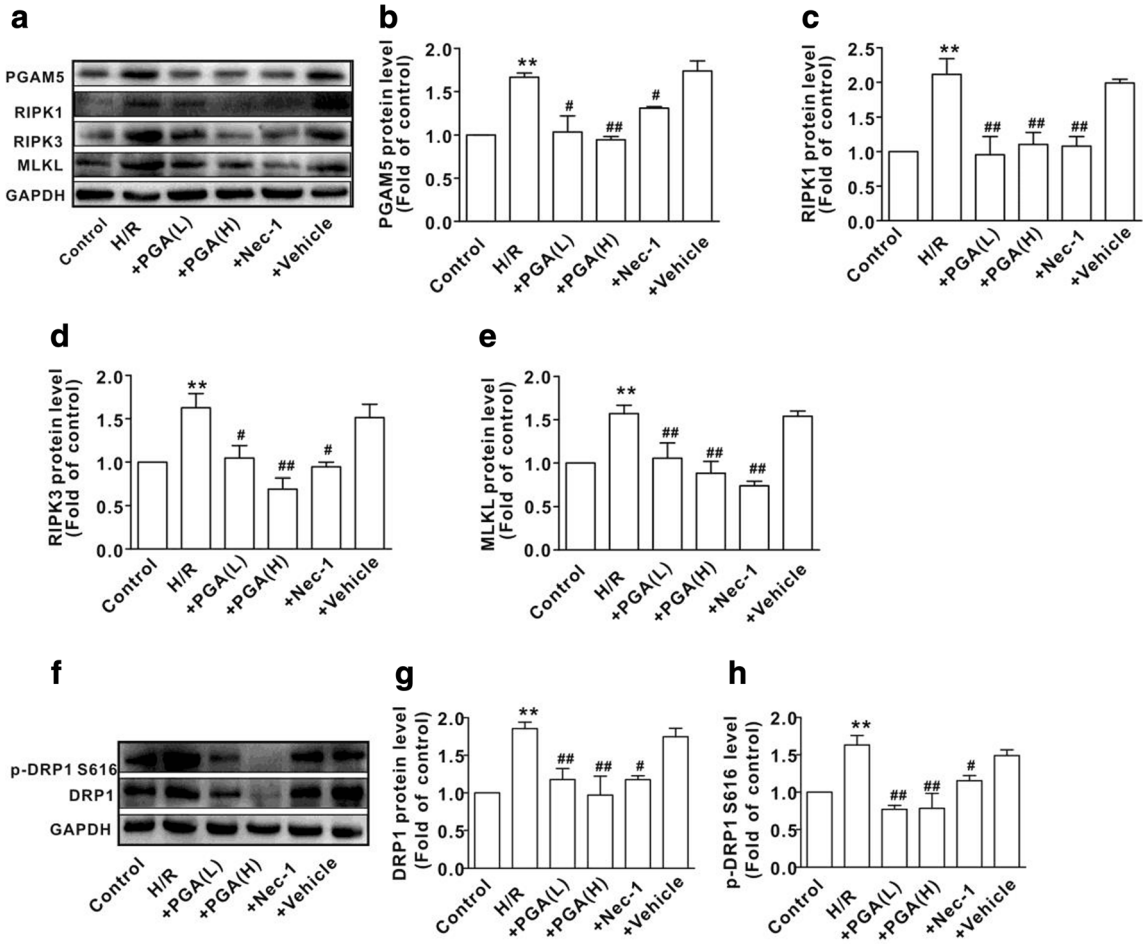

Fig. 4 Inhibition of PGAM5 decreases the levels of programmed necrosis-relevant proteins, DRP1, and p-DRP1-S616 in H/R-treated H9c2 cells. Arbitrary optical density units of the targeting protein were normalized against GAPDH and expressed as fold change. **a** Representative images of Western blot. **b** PGAM5 protein expression. **c** RIPK1 protein expression. **d** RIPK3 protein expression. **e** MLKL protein expression. **f** Representative images of Western blot. **g** DRP1 protein level. **h** p-DRP1-S616 protein level. All values were expressed as mean ± SEM (3 independent experiments in each group). H/R: hypoxia/reoxygenation; +PGA: H/R + phosphoglycolic acid; +Nec-1: H/R + necrostatin-1. $^{**}P < 0.01$ vs. control, $^{\#}P < 0.05$, $^{\#\#}P < 0.01$ vs. H/R

or siRNA negative control had little effect on the H/R-induced cellular necrosis.

Discussion

In this study, we explored the role of PGAM5 in regulation of RIPK-mediated myocardial necrosis in vivo or in vitro following I/R or H/R. Our results from in vivo and in vitro experiments showed that inhibition of PGAM5 (by PGA) or knockdown of PGAM5 expression (by siRNAs) obviously ameliorated I/R or H/R injury (such as the reduced infarct size and CK release or LDH release and cellular necrosis), together with downregulation of PGAM5, RIPK1, RIPK3, MLKL, Drp1, and p-Drp1, and the improved mitochondrial function (such as the decreased $\Delta\Psi m$ and ROS production). Interestingly, RIPK1 inhibitor (Nec-1) also achieved similar results to that of PGAM5 inhibitor (PGA). To the best of our knowledge, this study provide evidence for the first time that PGAM5 promotes necroptosis of cardiomyocytes following I/R or H/R through activation of mitochondrial fission protein Drp1.

For many years, necrosis was mostly considered to be a passive and accidental cell death resulting from severe damage to their structural integrity. The accidental and unregulated nature of necrosis means that it is deemed a difficult target for drug therapy [12]. Recently, the discovery of necrosis inhibitors and genetic evidence has changed this viewpoint since multiple pathways of regulated necrosis have been identified, such as necroptosis, ferroptosis, pyroptosis, oxytosis, and cyclophilin D–mediated necrosis [8, 11]. Among them, necroptosis is the best studied form of regulated necrosis. Although the molecular mechanisms for necrosis are not fully elucidated, the RIPK1/RIPK3/MLKL cascade is thought to mediate the necroptosis [25, 26]. Studies from different laboratories have demonstrated that RIPK-mediated necrosis

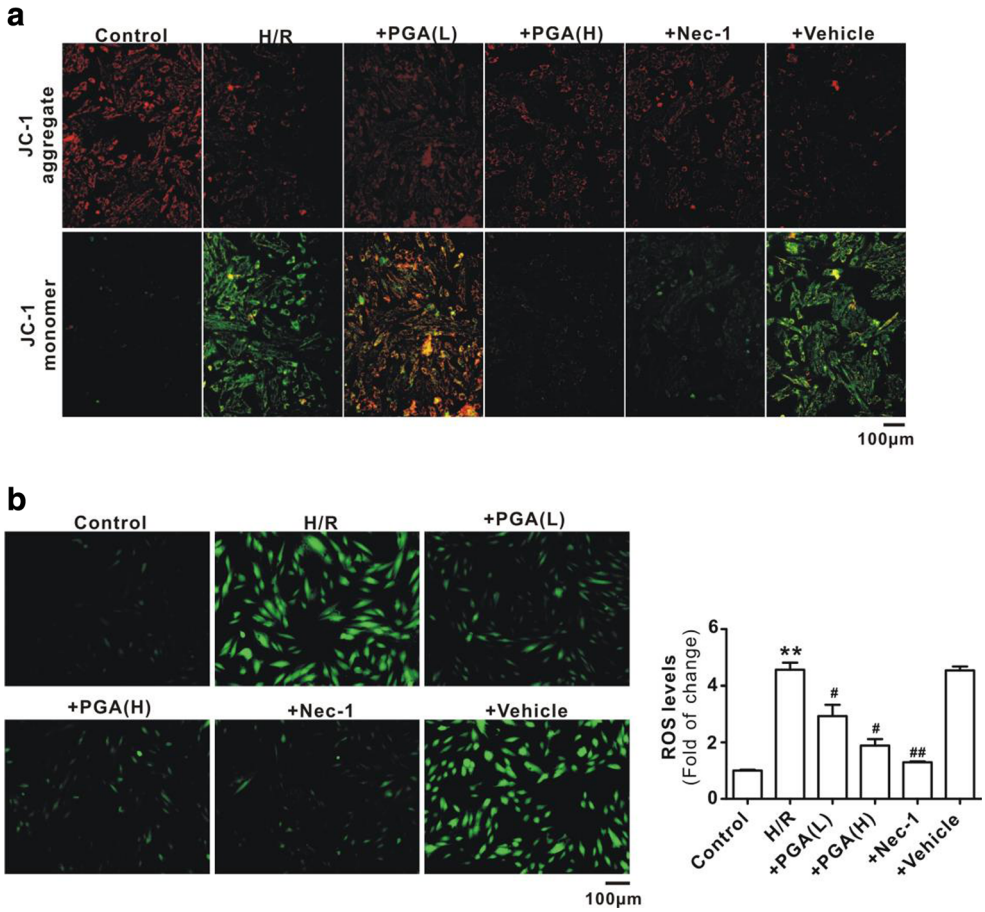

Fig. 5 Inhibition of PGAM5 improves mitochondrial function in H/R-treated H9c2 cells. **a** Representative images for mitochondrial membrane potential ($\Delta\Psi m$) assay in H9c2 cells. **b** Representative images for reactive oxygen species (ROS) assay in H9c2 cells (left), statistic value of fluorescent density for ROS in H9c2 cells (right). All values were expressed as mean ± SEM ($n = 6$ in each group). H/R: hypoxia/reoxygenation; +PGA: H/R + phosphoglycolic acid; +Nec-1: H/R + necrostatin-1. $^{**}P < 0.01$ vs. control, $^{\#}P < 0.05$, $^{\#\#}P < 0.01$ vs. H/R

accounted for, at least partially, the myocardial I/R injury. Suppression of RIPK1 by its inhibitor or relevant miRNAs was able to reduce the myocardial I/R injury [17, 19]. In the present study, we found that the protein expression of RIPK1, RIPK3, and MLKL in cardiac tissue or H9c2 cardiomyocyte was obviously upregulated following I/R or H/R, indicating that RIPK1/RIPK3/MLKL signaling pathway was involved in I/R- or H/R-induced myocardial necrosis. Administration of Nec-1 (the most frequently used RIPK1 inhibitor) could suppress the upregulation of RIPK1, RIPK3, and MLKL in I/R- or H/R-treated rat hearts or H9c2 cells together with a decrease in infarct size/CK release or LDH release/cellular necrosis. These results further verified the involvement of RIPK-dependent necrosis in myocardial I/R or H/R injury.

The knowledge relevant to necroptosis was mainly obtained by using RIPK1 inhibitors, such as Nec-1 [27], and animal models deficient in cognate members of necrosome, such as RIPK3 or MLKL [28]. Current efforts in prevention of necroptosis mainly focus on suppressing the activation of RIPK1, RIPK3, and/or MLKL, and Nec-1 is the most common option. Nec-1 was identified in 2005 due to its function in inhibition of TNF-α-induced necrotic cell death. After that, Nec-1 has been extensively used to explore the involvement of RIPK1-dependent necrosis [12]. However, some critical issues concerning the application of Nec-1 in vivo have emerged. Actually, Nec-1 is the same molecule as the indoleamine-2,3-dioxygenase (IDO) enzyme inhibitor: methyl-thiohydantoin-tryptophan [29]. Since IDO plays a key role in modulation of the innate and adaptive immune system, it cannot rule out the potential effect of Nec-1 on immune system. Therefore, its cardioprotective effect could be compromised. Furthermore, the dose-response curve of Nec-1 shows that it sensitizes mice to the lethality at low concentrations [30], suggesting that it is relatively toxic. For these reasons, Nec-1 is not considered an ideal drug for the prevention of myocardial I/R-induced necroptosis, and it is necessary to identify novel targets.

Recently, the mitochondrial phosphatase PGAM5 has been reported to function as the convergent point for multiple necrosis pathways [21], indicating that PGAM5 could be a novel therapeutic target against necroptosis. In TNF-α-induced necrosis of HeLa cells or HT-29 cells, RIPK1- and RIPK3-containing protein complexes were specifically formed in response to the necrosis induction, and PGAM5 was identified as a component of these complexes. Knockdown of PGAM5 expression in HT-29 cells or HeLa cells reduced necrosis about twofold, and the knockdown efficiency was correlated with the degree of necrosis rescue [21]. In another study, PGAM5(−/−) mice were used

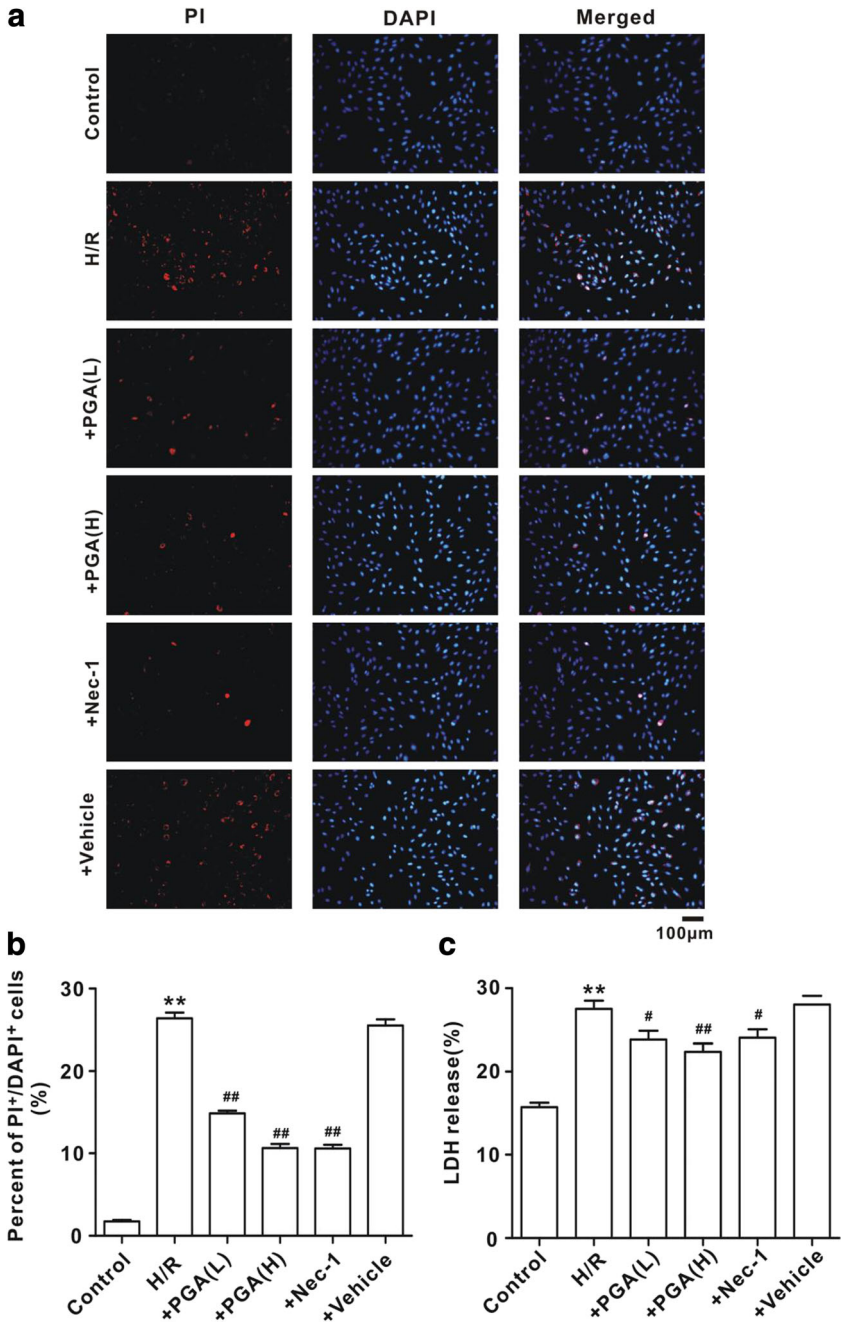

Fig. 6 Inhibition of PGAM5 decreases cellular necrosis in H/R-treated H9c2 cells. **a** Representative images for PI/DAPI double staining in H9c2 cells. **b** Percent of $PI^+/DAPI^+$ cells. **c** LDH release (indication for cellular damage) from H9c2 cells. All values were expressed as mean ± SEM ($n = 6$ in each group). H/R: hypoxia/reoxygenation; +PGA: H/R + phosphoglycolic acid; Nec-1: H/R + necrostatin-1. $^{**}P < 0.01$ vs. control, $^{\#}P < 0.05$, $^{\#\#}P < 0.01$ vs. H/R

for necrosis-mediated liver injury by intravenous administration of ConA [23], and deficiency of PGAM5 could protect the mice against ConA-induced liver injury compared to the ConA-treated wild-type mice. Histological analysis of liver tissue further verified the extensive necrotic cell death in wild-type but not in PGAM5-deficient mice. These reports provide evidence that PGAM5 is a key player in necroptosis. In our study, the results showed that PGAM5 protein expression in cardiac tissues or H9c2 cardiomyocytes was upregulated after I/R or H/R, accompanied by increases in infarct size/CK release or LDH release/cellular necrosis. These phenomena were mitigated by PGAM5 inhibitor (PGA) or PGAM5 siRNAs, suggesting that PGAM5 plays a key role in promotion of I/R- or H/R-induced necrosis.

According to a previous study, PGAM5 was able to recruit the mitochondrial fission protein Drp1 and activate it by dephosphorylation of Drp1 serine 637 (Drp1-S637) [21, 23, 31]. The activation of Drp1 causes mitochondrial fragmentation, an early and obligatory step for necrosis execution. Based on this report, we hypothesized that the mitochondrial phosphatase PGAM5 activates Drp1 through a decrease of p-Drp1-S637 level. Contrary to our hypothesis, the results showed that the levels of p-Drp1-S637 in I/R-treated hearts were not decreased, but it was

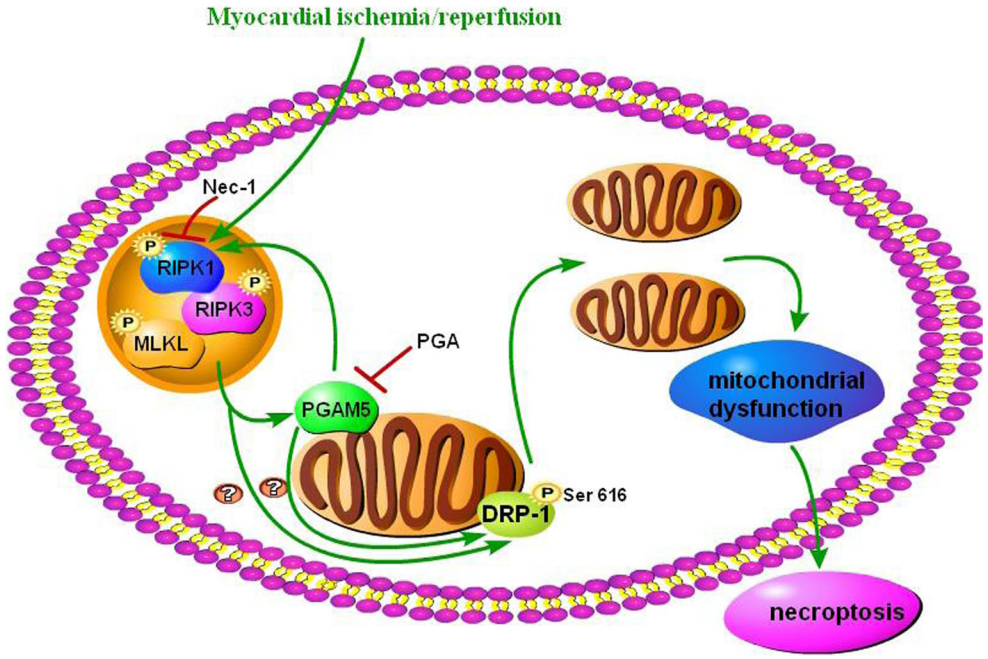

Fig. 7 Schematic diagram for illustrating the role of PGAM5 in promotion of necroptosis in I/R-treated rat hearts. Following myocardial I/R, the RIPK1/RIPK3/MLKL pathway is activated. As a direct target of RIPK3, PGAM5 is activated by RIPK3, but it also upregulates RIPK3, forming a positive feedback loop. The activation of RIPK1/RIPK3/MLKL pathway or PGAM5 accelerates mitochondrial fission by elevating Drp1 and p-Drp1-S616, resulting in mitochondrial dysfunction and necroptosis, which is blocked by RIPK1 or PGAM5 inhibitor. The downstream events linking Drp1-mediated mitochondrial fission after RIPK1/RIPK3/MLKL pathway or PGAM5 remain to be determined. I/R: ischemia/reperfusion; RIPK: receptor-interacting protein kinase; MLKL: mixed lineage kinase domain-like; PGAM5: phosphoglycerate mutase family member 5; Drp1: dynamin-related protein 1; Nec-1: necrostatin-1; PGA: phosphoglycolic acid

slightly elevated, albeit that PGAM5 was evidently upregulated. Different from Drp1-S637, phosphorylation of Drp1-S616 was able to activate Drp1 and accelerate mitochondrial fission, which causes mitochondrial dysfunction, a necessary step that drives the execution of necrotic cell death [23]. In this study, we have indeed found that the levels of p-Drp1-S616 in I/R- or H/R-treated hearts or H9c2 cells were obviously elevated concomitant with mitochondrial dysfunction; these effects were attenuated by inhibition of PGAM5 or knockdown of PGAM5 expression, indicating that the activation of Drp1 is not directly dependent on the phosphatase activity of PGAM5.

Based on the report on the correlation between PGAM5 and necroptosis, PGAM5 is at the downstream of RIPK1/RIPK3/MLKL pathway [21, 31], and inhibition of RIPK1 could lead to downregulation of PGAM5. In the present study, our results showed that there was a similar change in protein levels between RIPK1 and PGAM5 in I/R-treated rat hearts or H/R-treated H9c2 cells, and inhibition of RIPK1 downregulated RIPK1, RIPK3, MLKL, PGAM5, and p-Drp1-S616. Interestingly, inhibition or knockdown of PGAM5 also achieved the same results. Based on these observations, we thus think there is a positive feedback between RIPK1 and PGAM5 (Fig. 7). However, the downstream signaling pathways and events linking Drp1-mediated mitochondrial fission to necrosis remain to be determined.

In summary, our findings demonstrated for the first time that inhibition of PGAM5 could reduce I/R-induced necroptosis in rat hearts through suppression of mitochondrial fission protein Drp1, and there is a positive feedback between RIPK1 and PGAM5. Although PGAM5 may have the potentials to serve as a novel therapeutic target for prevention of myocardial I/R injury, more studies with functional assessment and clinical data are needed before confirming its therapeutic relevance.

Funding This work was supported by the National Natural Science Foundation of China (No. 81872873 to Jun Peng; No. 81573430 to Xiu-Ju Luo; No. 81703516 to Bin Liu).

Compliance with Ethical Standards

Conflict of Interest The authors declare that they have no conflict of interest.

Ethical Approval All applicable international, national, and/or institutional guidelines for the care and use of animals were followed.

Publisher's Note Springer Nature remains neutral with regard to jurisdictional claims in published maps and institutional affiliations.

References

1. He X, Li S, Liu B, Susperreguy S, Formoso K, Yao J, et al. Major contribution of the 3/6/7 class of TRPC channels to myocardial ischemia/reperfusion and cellular hypoxia/reoxygenation injuries. Proc Natl Acad Sci U S A. 2017;114(23):E4582–e91.
2. Harisseh R, Pillot B, Gharib A, Augeul L, Gallo-Bona N, Ferrera R, et al. Unacylated ghrelin analog prevents myocardial reperfusion injury independently of permeability transition pore. Basic Res Cardiol. 2017;112(1):4.
3. Yang C, Liu X, Yang F, Zhang W, Chen Z, Yan D, et al. Mitochondrial phosphatase PGAM5 regulates Keap1-mediated Bcl-xL degradation and controls cardiomyocyte apoptosis driven by myocardial ischemia/reperfusion injury. In vitro cellular & developmental biology. Animal. 2017;53(3):248–57.
4. Orrenius S, Zhivotovsky B, Nicotera P. Regulation of cell death: the calcium-apoptosis link. Nature reviews. Mol Cell Biol. 2003;4(7):552–65.
5. Elmore S. Apoptosis: a review of programmed cell death. Toxicol Pathol. 2007;35(4):495–516.
6. Adameova A, Goncalvesova E, Szobi A, Dhalla NS. Necroptotic cell death in failing heart: relevance and proposed mechanisms. Heart Fail Rev. 2016;21(2):213–21.
7. Fietta P. Many ways to die: passive and active cell death styles. Riv Biol. 2006;99(1):69–83.
8. Ying Y, Padanilam BJ. Regulation of necrotic cell death: p53, PARP1 and cyclophilin D-overlapping pathways of regulated necrosis? Cell Mol Life Sci. 2016;73(11–12):2309–24.
9. Tonnus W, Linkermann A. The in vivo evidence for regulated necrosis. Immunol Rev. 2017;277(1):128–49.
10. Ashkenazi A, Salvesen G. Regulated cell death: signaling and mechanisms. Annu Rev Cell Dev Biol. 2014;30:337–56.
11. Vanden Berghe T, Linkermann A, Jouan-Lanhouet S, Walczak H, Vandenabeele P. Regulated necrosis: the expanding network of non-apoptotic cell death pathways. Nature reviews. Mol Cell Biol. 2014;15(2):135–47.
12. Conrad M, Angeli JP, Vandenabeele P, Stockwell BR. Regulated necrosis: disease relevance and therapeutic opportunities. Nature reviews. Drug Discov. 2016;15(5):348–66.
13. Grootjans S, Vanden Berghe T, Vandenabeele P. Initiation and execution mechanisms of necroptosis: an overview. Cell Death Differ. 2017;24(7):1184–95.
14. Linkermann A, Brasen JH, Darding M, Jin MK, Sanz AB, Heller JO, et al. Two independent pathways of regulated necrosis mediate ischemia-reperfusion injury. Proc Natl Acad Sci U S A. 2013;110(29):12024–9.
15. Hussain M, Zimmermann V, van Wijk SJL, Fulda S. Mouse lung fibroblasts are highly susceptible to necroptosis in a reactive oxygen species-dependent manner. Biochem Pharmacol. 2018;153:242–7.
16. Schreiber A, Rousselle A, Becker JU, von Massenhausen A, Linkermann A, Kettritz R. Necroptosis controls NET generation and mediates complement activation, endothelial damage, and autoimmune vasculitis. Proc Natl Acad Sci U S A. 2017;114(45):E9618–e25.
17. Qin D, Wang X, Li Y, Yang L, Wang R, Peng J, et al. MicroRNA-223-5p and -3p cooperatively suppress necroptosis in ischemic/reperfused hearts. J Biol Chem. 2016;291(38):20247–59.
18. Wang K, Liu F, Liu CY, An T, Zhang J, Zhou LY, et al. The long noncoding RNA NRF regulates programmed necrosis and myocardial injury during ischemia and reperfusion by targeting miR-873. Cell Death Differ. 2016;23(8):1394–405.
19. Oerlemans MI, Liu J, Arslan F, den Ouden K, van Middelaar BJ, Doevendans PA, et al. Inhibition of RIP1-dependent necrosis prevents adverse cardiac remodeling after myocardial ischemia-reperfusion in vivo. Basic Res Cardiol. 2012;107(4):270.
20. Wang JX, Zhang XJ, Li Q, Wang K, Wang Y, Jiao JQ, et al. MicroRNA-103/107 regulate programmed necrosis and myocardial ischemia/reperfusion injury through targeting FADD. Circ Res. 2015;117(4):352–63.
21. Wang Z, Jiang H, Chen S, Du F, Wang X. The mitochondrial phosphatase PGAM5 functions at the convergence point of multiple necrotic death pathways. Cell. 2012;148(1–2):228–43.
22. Chaikuad A, Filippakopoulos P, Marcsisin SR, Picaud S, Schroder M, Sekine S, et al. Structures of PGAM5 provide insight into active site plasticity and multimeric assembly. Structure (London, England: 1993). 2017;25(7):1089–99.e3.
23. He GW, Gunther C, Kremer AE, Thonn V, Amann K, Poremba C, et al. PGAM5-mediated programmed necrosis of hepatocytes drives acute liver injury. Gut. 2017;66(4):716–23.
24. Zhang YS, He L, Liu B, Li NS, Luo XJ, Hu CP, et al. A novel pathway of NADPH oxidase/vascular peroxidase 1 in mediating oxidative injury following ischemia-reperfusion. Basic Res Cardiol. 2012;107(3):266.
25. Chen S, Lv X, Hu B, Shao Z, Wang B, Ma K, et al. RIPK1/RIPK3/MLKL-mediated necroptosis contributes to compression-induced rat nucleus pulposus cells death. Apoptosis. 2017;22(5):626–38.
26. Shen C, Wang C, Han S, Wang Z, Dong Z, Zhao X, et al. Aldehyde dehydrogenase 2 deficiency negates chronic low-to-moderate alcohol consumption-induced cardioprotection possibly via ROS-dependent apoptosis and RIP1/RIP3/MLKL-mediated necroptosis. Biochim Biophys Acta. 2017;1863(8):1912–8.
27. Takahashi N, Duprez L, Grootjans S, Cauwels A, Nerinckx W, DuHadaway JB, et al. Necrostatin-1 analogues: critical issues on the specificity, activity and in vivo use in experimental disease models. Cell Death Dis. 2012;3:e437.
28. Welz PS, Wullaert A, Vlantis K, Kondylis V, Fernandez-Majada V, Ermolaeva M, et al. FADD prevents RIP3-mediated epithelial cell necrosis and chronic intestinal inflammation. Nature. 2011;477(7364):330–4.
29. Vandenabeele P, Grootjans S, Callewaert N, Takahashi N. Necrostatin-1 blocks both RIPK1 and IDO: consequences for the study of cell death in experimental disease models. Cell Death Differ. 2013;20(2):185–7.
30. Degterev A, Maki JL, Yuan J. Activity and specificity of necrostatin-1, small-molecule inhibitor of RIP1 kinase. Cell Death Differ. 2013;20(2):366.
31. Kang YJ, Bang BR, Han KH, Hong L, Shim EJ, Ma J, et al. Regulation of NKT cell-mediated immune responses to tumours and liver inflammation by mitochondrial PGAM5-Drp1 signalling. Nat Commun. 2015;6:8371.